REACTION EXPERIMENTS FOR THERMOCHEMICAL WATER-SPLITTING

John Gahimer, Jon Pangborn, Stephan Foh,
Mono Mazumder, and Robert Stotz

Institute of Gas Technology
3424 South State Street
Chicago, Illinois 60616

INTRODUCTION

A thermochemical water-splitting process is a sequence of chemical reactions in which every species except water is recycled. Ideally, the net inputs are only water and thermal energy. The net outputs are hydrogen, oxygen, and degraded heat. Thermochemical water-splitting processes offer a closed-cycle, non-material-polluting route to fuel synthesis. They are environmentally compatible because the only by-product is oxygen and because combustion of the product hydrogen re-creates the raw material, water.

In the long term, thermochemical water-splitting processes offer a conversion technology for transforming heat from any moderate- or high-temperature source into chemical energy by using a perpetually available resource. For the near term, hydrogen from a heat source, such as a nuclear reactor, can be used to supplement fossil-fuel sources such as natural gas (blending), petroleum (hydrotreating), and especially coal, shale kerogens, or sand bitumens (hydrogenation to liquids or gases). The American Gas Association is sponsoring a program, now in its fifth year at the Institute of Gas Technology, to theoretically and experimentally evaluate thermochemical water-splitting as a method of fuel production. If hydrogen and oxygen can be produced by a water-splitting process at low cost, they would assume increased importance as industrial commodities as well as fuel sources.

Ideally, water can be split into hydrogen and oxygen by supplying the enthalpy of reaction with a combination of thermal energy (for entropy requirements) and work energy (for free-energy requirements). The present technology for water-splitting is electrolysis, in which work energy (electricity) in excess of the reaction enthalpy is supplied to produce hydrogen and oxygen from a water-electrolyte solution. A heat-to-work transformation is needed to generate the required electrical energy from primary thermal energy (fossil, nuclear, or solar). The efficiency of this transformation is restricted by thermodynamic limitations and by practical constraints in operating power plants. Photolysis processes will encounter a similar restriction if the light is produced from thermal primary energy. Direct solar energy input to photolysis seems limited by the small fraction of the solar spectrum that has sufficient energy, per photon, to drive known photolytic reactions.

To reduce the requirement for a heat-to-work cycle, water can be decomposed in a single step by heating it to very high temperatures (2500° to 4000°C) and separating the gaseous products. The materials required for containment and separation obviously limit practical applications at these temperatures. The same thermal decomposition and separation can be accomplished through multiple chemical reaction steps operating at lower temperatures, i.e., through a thermochemical water-splitting process. According to the second law of thermodynamics, quantities of heat in excess of the reaction free energy plus entropy requirements of water-splitting must be supplied. The chemical reactions are

driven primarily by heat inputs, with minimal process work (mechanical and electrical) requirements. Research at IGT has emphasized these processes, for which the predominant form of energy input is heat, with the expectation of more efficient and less capital-intensive processes than those depending primarily upon conversions of heat to work, such as electrolysis.

CLASSES OF KNOWN CYCLES

Nearly all the (pure) thermochemical water-splitting cycles (i.e., closed-loop reaction sequences operated predominantly with thermal energy inputs) published to date (1) can be grouped into one of the five generic classes shown in Table 1.

Table 1. CLASSES OF KNOWN THERMOCHEMICAL HYDROGEN PRODUCTION CYCLES

Class 1: Metal-Metal Oxide Cycles

$$M + H_2O \rightarrow MO + H_2$$
$$MO \rightarrow M + 1/2\,O_2$$

Class 2: Metal Oxide-Metal Hydroxide Cycles

$$M + 2H_2O \rightarrow M(OH)_2 + H_2$$
$$M(OH)_2 \rightarrow MO + H_2O$$
$$MO \rightarrow M + 1/2\,O_2$$

Class 3: Metal Oxide-Metal Sulfate Cycles

$$MO + SO_2 + H_2O \rightarrow MSO_4 + H_2$$
$$MSO_4 \rightarrow MO + SO_3$$
$$SO_3 \rightarrow SO_2 + 1/2\,O_2$$

Class 4: Metal-Metal Halide Cycles

$$M + 2HX \rightarrow MX_2 + H_2$$
$$MX_2 \rightarrow M + X_2$$
$$X_2 + H_2O \rightarrow 2HX + 1/2\,O_2$$

Class 5: Metal Oxide-Metal Halide Cycles

$$M + H_2O \rightarrow MO + H_2$$
$$MO + 2HX \rightarrow MX_2 + H_2O$$
$$MX_2 \rightarrow M + X_2$$
$$X_2 + H_2O \rightarrow 2HX + 1/2\,O_2$$

(In this table, M can be interpreted as either a zero-valent metal or the lower valance state of an oxide pair or halide pair.) Of course, other types of cycles are possible for hybrid electrothermochemical cycles that include one or more electrolytic steps with work energy (electricity) input. Other types of cycles can also be derived for other forms of work energy input, such as photolysis.

Of course, myriad combinations of these five classes can be made. In general, however, the simpler schemes are expected to be more desirable in terms of both efficiency and capital cost.

No two-step thermochemical cycles, the metal-metal oxide cycles (Class 1 in Table 1) are known to be operable within the temperature range of interest for this program, 300° to 1200°K. Two-step cycles theoretically might be constructed from metal-metal hydride pairs; none have been reported. Many compounds theoretically can form three-step cycles of the metal oxide-metal hydroxide Class 2 or the metal oxide-metal sulfate Class 3. The sulfuric acid cycle investigated by Bowman et al. at Los Alamos Scientific Laboratory (2) and by Brecher et al. at Westinghouse Electric Corp. (3) could be considered a member of both Class 2 with M = sulfur dioxide and of Class 3 with MO = water.

The metal-metal halide Class 4, as written in Table 1, is viable only for chlorides and fluorides because bromine and iodine have unfavorable equilibria in the halogen-steam reaction (the analog of the reverse-Deacon reacton. Because the metal fluorides are relatively stable, cycles involving them are usually not very energy efficient, and fluorine and hydrogen fluoride present obvious containment problems at high temperatures. Thus the chlorides are most practical. Except for rare earth compounds, the only metal-metal chloride pair that we have found to be thermodynamically feasible in three-step cycles of Class 4 (for the 300° to 1200°K temperature envelope available from an HTGR nuclear heat source) is $CrCl_2$-$CrCl_3$.

Some specific examples of chemical reaction sequences for these five generic classes of thermochemical water-splitting cycles are shown in Table 2, along with temperatures at which the reactions should theoretically proceed. Also tabulated are the Gibbs' free-energy change and enthalpy change for each reaction at the stated temperature, and calculated "maximum attainable" energy efficiency for each cycle based on the stated temperature sequence, assuming only near-term technology. "Maximum attainable" energy efficiency is our nomenclature for a figure of merit which is the upper limit of the process flowsheet efficiency calculation. Our efficiency calculation methodology has been discussed in previous papers (4, 20).

Several methods of calculating cycle efficiencies have been proposed (9-13). The IGT method assumes that all primary input energy is heat and that the product energy is the high heating value of the hydrogen produced. It is based on an energy and material balance for the cycle, and it takes into account the work terms due to poor reaction yields and reactant recycles, gas separations, electrochemical steps, and compressions, with a credit for work generated from excess heat available at greater than 600°K. Heat exchange within the cycle is optimized by inspection. Thermodynamic quantities are taken or calculated from standard reference works on the thermodynamic properties of materials (5-8). A computer program utilizing essentially the same methodology has been developed by the University of Kentucky (11). (This program gives somewhat lower values for cycle efficiency than does IGT's calculation because of differences in the pattern of internal heat transfer and assumptions about the efficiency of generating work from heat.)

The example cycles shown in Table 2 are in the high end of the efficiency range we have found for feasible thermochemical cycles, with "maximum attainable" efficiencies ranging from 47% to 65%. They illustrate the general trend that cycles with few steps and high input temperatures have higher efficiencies, as expected, and that thermodynamically feasible and efficient cycles, for the 300° to 1500°K temperature span, usually have individual reaction steps whose Gibbs' free-energy change is in the range of about −15 to about +15 kilocalories.

Table 2. EXAMPLES OF KNOWN THERMOCHEMICAL HYDROGEN PRODUCTION CYCLES

	Temp, °K	G_T^o, kcal	H_T^o, kcal
Metal-Metal Oxide Cycle L-1 (65% "Maximum Attainable" Efficiency)			
$Cd(s) + H_2O(g) \rightarrow CdO(s) + H_2(g)$	400	+1.8	−3.1
$CdO(s) \rightarrow Cd(g) + 1/2\,O_2(g)$	1500	+8.7	+84.8
Metal Oxide-Metal Hydroxide Cycle L-2 (65% "Maximum Attainable" Efficiency)			
$Cd(s) + 2H_2O(\ell) \rightarrow Cd(OH)_2(s) + H_2(g)$	Electrolysis	+1.0	+3.4
$Cd(OH)_2(s) \rightarrow CdO(s) + H_2O(g)$	650	0.0	+12.3
$CdO(s) \rightarrow Cd(g) + 1/2\,O_2(g)$	1500	+8.7	+84.8
Metal Oxide-Metal Sulfate Cycle C-7 (57% "Maximum Attainable" Efficiency)			
$Fe_2O_3(s) + 2SO_2(g) + H_2O(g) \rightarrow 2FeSO_4(s) + H_2(g)$	400	−8.8	−46.6
$2FeSO_4(s) \rightarrow Fe_2O_3(s) + SO_2(g) + SO_3(g)$	1000	−0.9	+78.8
$SO_3(g) \rightarrow SO_2(g) + 1/2\,O_2(g)$	1200	−3.3	+23.1
Metal-Metal Halide Cycle J-1 (47% "Maximum Attainable" Efficiency)			
$2CrCl_2(s) + 2HCl(g) \rightarrow 2CrCl_3(s) + H_2(g)$	600	0.0	−30.8
$2CrCl_3(s) \rightarrow 2CrCl_2(\ell) + Cl_2(g)$	1200	+15.1	+86.5
$Cl_2(g) + H_2O(g) \rightarrow 2HCl(g) + 1/2\,O_2(g)$	1200	−5.4	+14.2
Metal Oxide-Metal Halide Cycle B-1 (47% "Maximum Attainable" Efficiency)			
$3FeCl_2(\ell) + 4H_2O(g) \rightarrow Fe_3O_4(s) + 6HCl(g) + H_2(g)$	1200	−0.3	+45.8
$Fe_3O_4(s) + 8HCl(g) \rightarrow 2FeCl_3(s) + FeCl_2(s) + 4H_2O(g)$	400	−13.4	−58.8
$2FeCl_3(s, g) \rightarrow 2FeCl_2(s) + Cl_2(g)$	700	−5.7	−37.8
$Cl_2(g) + H_2O(g) \rightarrow 2HCl(g) + 1/2\,O_2(g)$	1200	−5.4	+14.2

From the examples in Table 2, we can also conclude that thermochemical water-splitting is potentially a very efficient technology for transforming primary heat energy into secondary fuel energy. IGT has theoretically examined about 150 specific examples of such cycles. Of these, about 90 are thermodynamically feasible and about 60 meet our criteria for warranting some experimental work ("maximum attainable" efficiency greater than 35% and no compounds of unmanageable corrosivity).

EXPERIMENTAL OBJECTIVE AND PROCEDURES

The experimental objective is to determine which cycles are technically feasible and whether their efficiency is still attractive at actual operating conditions. Thus, our experimental program examines the reaction steps of theoretically possible and potentially efficient cycles to identify those that are truly workable. Undocumented reaction steps are tested in the laboratory to determine feasibility, practicality, and yields at operating conditions. Documented reaction steps are verified, including operating conditions different from those reported in the literature, and the morphology of solid products is determined.

Our purpose is to prove the feasibility of performing certain chemical reactions by supplying primarily heat energy. Reactions that require excessive work energy are undesirable; therefore, we usually construct uncomplicated reaction systems that do not involve mixing or fluidization. In the preliminary reaction trials reported here, total pressure is always about 1 atmosphere.

Our standard procedure is to expose 5 to 50 grams of solid or liquid reactant, in an inert ceramic boat or in a packed bed, to a continuous flow of gaseous reactant or inert carrier gas. The systems are operated as batch reactors (for solid materials) with gaseous product removal. All materials exposed to the reaction are glass, quartz, or ceramic. When a 25% or more conversion (mole basis) occurs in 1 to 2 hours with reagent-grade reactants, we consider that reaction to be proved "workable." When all the reactions of a cycle are proved workable with reagent-grade materials, and we have operated the entire cycle, step by step, with recycled materials, we consider that cycle to be "demonstrated."

THE GROUP OF IRON-CHLORINE-HYDROGEN-OXYGEN CYCLES

Of the 150 cycles that we have theoretically examined, only 12 are experimentally workable with reagent-grade materials, and only four of these have been demonstrated with recycled materials. To our knowledge, another five cycles have been shown to be experimentally workable by other research groups, and we understand that one of these has been demonstrated (19). Interestingly, of this total of 17 known workable cycles, 12 belong to the group of metal oxide-metal halide cycles (Class 5 in Table 1) that are constructed from the elements iron-chlorine-hydrogen-oxygen. The nine chemical reactions shown in Table 3 are sufficient to construct five of these 12 cycles. The other seven known cycles of this group involve substituting two reactions for one of those listed or combining two reactions into one.

The following discussion of our experimental results is organized into four functional sections: metal oxidation (Reactions 1 and 2), metal halogenation (Reactions 3, 4, and 5), metal reduction (Reactions 6 and 7), and halogen recycle (Reactions 8 and 9).

Table 3. REACTIONS OF THE IRON-CHLORINE-HYDROGEN-OXYGEN GROUP OF CYCLES

No.		T, °K	ΔG_T^0, kcal	ΔH_T^0, kcal	Cycles
	Metal Oxidation				
1	$3Fe(s) + 4H_2O(g) \rightarrow Fe_3O_4(s) + 4H_2(g)$	800	−9.3	−26.7	A-1, A-2
2	$3FeCl_2(s) + 4H_2O(g) \rightarrow Fe_3O_4(s) + 6HCl(g) + H_2(g)$	1200	−0.3	+45.8	B-1, B-2, I-6
	Metal Halogenation				
3	$Fe_3O_4(s) + 8HCl(g) \rightarrow 2FeCl_3(s) + FeCl_2(s) + 4H_2O(g)$	400	−13.4	−58.8	A-1, B-1
4	$Fe_3O_4(s) + 9/2\ Cl_2(g) \rightarrow 3FeCl_3(g) + 2O_2(g)$	1200	+11.1	+73.0	A-2, B-2
5	$Fe_3O_4(s) + 3/2\ Cl_2(g) + 6HCl(g) \rightarrow 3FeCl_3(s) + 3H_2O(g) + 1/2\ O_2(g)$	400	−11.4	−65.3	I-6
	Metal Reduction				
6	$2FeCl_3(s) \rightarrow 2FeCl_2(s) + Cl_2(g)$	700	−5.7	−37.8	A-1, A-2, B-1, B-2, I-6
7	$3FeCl_2(\ell) + 3H_2(g) \rightarrow 3Fe(s) + 6HCl(g)$	1200	+1.4	+71.3	A-1, A-2
	Halogen Recycle				
8	$Cl_2(g) + H_2O(g) \rightarrow 2HCl(g) + 1/2\ O_2(g)$	1200	−5.4	−14.2	A-1, B-1
9	$6HCl(g) + 3/2\ O_2(g) \rightarrow 3Cl_2(g) + 3H_2O(g)$	400	−22.5	−41.3	A-2, B-2

METAL OXIDATION

Reactions 1 and 2 are the hydrogen-producing steps of these cycles, i.e., the reduction of steam to molecular hydrogen by using steam to oxidize a metal or metal halide species. We would theoretically prefer to make Fe_2O_3 in either reaction, since it would produce more hydrogen per unit of solid, but the more stable Fe_3O_4 predominates. The Fe_2O_3 probably offers only a theoretical, not a real, advantage because the kinetics of the subsequent halogenation reaction are slower with Fe_2O_3 than with Fe_3O_4.

1) $$3Fe + 4H_2O \rightarrow Fe_3O_4 + 4H_2$$

The steam-iron reaction is well-known industrial technology. A modern, continuous version of it is the hydrogen-producing step in one variation of IGT's HYGAS Process for the synthesis of pipeline gas from coal (15-17). The free-energy change for this reaction is favorable over the entire temperature span of interest, as shown in Figure 1. Our experimental tests found a minimum useful temperature of 600°C, where 44% conversion was obtained. Greater conversions can be obtained at higher temperatures because of improved reaction kinetics. The reaction conversion also depends on iron morphology.

2) $$3FeCl_2 + 4H_2O \rightarrow Fe_3O_4 + 6HCl + H_2$$

For the steam-$FeCl_2$ reaction, free-energy changes (Figure 1) are negative only above 920°C. However, the reaction proceeds to some extent at 400°C, with excess steam flow and continuous removal of HCl and hydrogen; the solid product is a mixture of Fe_3O_4, Fe_2O_3, and FeOCl. At higher temperatures, higher yields of Fe_3O_4 and higher total conversions are noted. Essentially complete conversion to oxides occurs in less than 2 hours at 600°C (again, with excess steam flow). No undesired side reactions are observed, but significant quantities of FeOCl are produced, particularly at temperatures below 600°C, if the reaction is stopped short of completion. Apparently the oxychloride is an intermediate product; it vanishes if reacted further with steam at the higher temperatures.

The Appendix details a new method of analysis that we have developed for the iron oxides.

METAL HALOGENATION

Reactions 3 and 4 are metal halogenation, the reaction of metal oxide with halogen or halogen acid to produce metal halide. A simple substitution of chloride for oxide occurs in Reaction 3; in Reaction 4, one of the three iron atoms is oxidized. Reaction 5 is a combination of halogenation and halogen recycle; it performs the functions of both Reaction 4 and Reaction 9. These reactions, particularly 4 and 5, can also be viewed as the oxygen release reactions.

3) $$Fe_3O_4 + 8HCl \rightarrow 2FeCl_3 + FeCl_2 + 4H_2O$$

Based on the free-energy change for Reaction 3 (Figure 2), reasonable reaction yields are expected and observed at temperatures below 250°C. In a vertical, packed-bed reactor with slight excess HCl flow, Reaction 3 proceeds to complete conversion in 2 to 5 hours over the entire temperature span 200° to 400°C. Stoichiometry of the condensed products agrees with stoichiometry of Reaction 3, indicating that the $FeCl_3$ decomposition, Reaction 6, does not proceed concurrently at this temperature when excess HCl is present.

The gases evolved from the reaction are HCl , excess H_2O , and the dimer, Fe_2Cl_6. Small quantities of FeOCl also are present, depending on operating conditions. If the Fe_2Cl_6 is allowed to solidify in the presence of condensing steam, a hydrate is formed. Dehydration of the $FeCl_3$ hydrate is difficult and usually results in the formation of Fe_2O_3, which is not desirable at this step in the cycles. Because of this, we normally operate this reactor with an exit zone where the temperature is only slightly greater than 100°C, and the Fe_2Cl_6 solidifies in this zone.

4) $$Fe_3O_4 + 9/2\,Cl_2 \rightarrow 3FeCl_3 + 2O_2$$

The free-energy change of Reaction 4 (Figure 2) decreases continuously with increasing temperature. Although the equilibrium is quite unfavorable above 725°C, the reaction does proceed significantly at these temperatures with excess chlorine flow and continuous removal of the gaseous Fe_2Cl_6 and oxygen products. Conversions of 26% in 2 hours were observed at temperatures as low as 800°C. Complete conversion was obtained in 5 hours at 925°C. Chlorine gas, being a stronger oxidizing agent than HCl, produces only $FeCl_3$ as an iron-containing product, whereas in Reaction 3, both $FeCl_3$ and $FeCl_2$ are produced. Concurrent decomposition of $FeCl_3$ occurs neither in the presence of chlorine for Reaction 4, at these temperatures, nor in the presence of HCl for Reaction 3.

5) $$Fe_3O_4 + 3/2Cl_2 + 6HCl \rightarrow 3FeCl_3 + 3H_2O + 1/2\,O_2$$

Figure 2 shows that Reaction 5 is thermodynamically favored at temperatures below 225°C. We find essentially complete conversion from 125° to 200°C in a packed-bed reactor with downflow of excess gaseous reactants and continuous removal of gaseous products. The product analyses do not match the reaction stoichiometry as written. For instance, in the trial at 150°C, the product solids were 80 mole % $FeCl_3$ and 20 mole % FeOCl.

In these experiments the reactant gases, chlorine and HCl,in the correct stoichiometric ratio are metered into the reaction zone together. The reaction zone contains a moderate vapor pressure of the gaseous dimer, Fe_2Cl_6, from the $FeCl_3$ reaction product, and some of this dimer passes downward through the packed bed along with the other gaseous reaction products. Below the solid bed, an exit temperature zone of slightly above 100°C is maintained to solidify the Fe_2Cl_6 without allowing steam condensation; however, we always find FeOCl in the solid product below the bed. Experimental configurations without the intermediate temperature zone produce more FeOCl. By removing the FeOCl and further treating it with HCl or chlorine gas, the FeOCl can be converted to $FeCl_3$, maintaining a closed cycle.

METAL REDUCTION

Reactions 6 and 7 are halide decomposition and the reaction of halide with hydrogen to produce metal. They reduce the metal atom oxidation state, and they are the most difficult steps to operate experimentally. This difficulty is not surprising because the product of these reactions must be capable of reducing water to molecular hydrogen. As shown in Figure 3, Reaction 7 is thermodynamically favored only at temperatures above about 950°C, and Reaction 6 is favored only in a narrow temperature range (700° to 800°K). Even this is an oversimplification for Reaction 6, because the competing reaction of $FeCl_3$ to gaseous dimer is significant at these temperatures.

6) $$2FeCl_3(s) \rightarrow 2FeCl_2(s) + Cl_2(g)$$

Because of the competing favorable equilibrium of $FeCl_3$ to the relatively more stable gaseous dimer Fe_2Cl_6 and the quite unfavorable equilibrium of the

dimer-to-$FeCl_2$ reaction, Reaction 6 exhibits poor yields when operated by normal techniques. The dimer is present over the entire temperature range of interest. Although $FeCl_3$ has a boiling point of 332°C and a melting point of 302°C, we have observed formation of the gaseous dimer (by sublimation) at temperatures as low as 225°C. In a horizontal reactor with inert gas flow, the conversion to $FeCl_2$ is less than 5%. In a system with no external flow, purged initially with inert gas and with a cooled exit open to atmospheric pressure, we find slightly improved conversions of 9.5% down to 2.1% over the temperature span 225° to 500°C. By repeated cycling of material, the best overall yield is about 20% in 5 hours.

Reaction 6 can be replaced by a pair of reactions that perform the same function:

$$FeCl_3 + CuCl \rightarrow FeCl_2 + CuCl_2$$

$$CuCl_2 \rightarrow CuCl + 1/2Cl_2$$

The first reaction is performed by placing a layer of CuCl in stoichiometric excess on top of a layer of $FeCl_3$. As expected from reaction free-energy change calculations, the reaction proceeds at temperatures below 290°C. Complete conversion is obtained at 280°C in 2 hours. Only slight traces of $FeCl_3$ escape the CuCl layer.

The second reaction is more complicated, because $FeCl_2$ and $CuCl_2$ cannot be easily separated. The reaction is thermodynamically favored above 500°C, but when the mixture from the first reaction is heated to this temperature the products are $FeCl_3$ and CuCl. Temperature staging allows the decomposition of $CuCl_2$ to proceed with minimum concurrent reoxidation of the $FeCl_2$. At temperatures of 275° to 325°C, the following reaction occurs:

$$10FeCl_2 + 10CuCl_2 \rightarrow 7FeCl_3 + 3FeCl_2 + 10CuCl + 3/2Cl_2$$

After chlorine has been swept from the reaction zone, the products can be reduced in temperature and the first reaction repeated to yield:

$$7FeCl_3 + 3FeCl_2 + 10CuCl \rightarrow 10FeCl_2 + 7CuCl_2 + 3CuCl$$

If these two reactions are cycled repeatedly with chlorine removal, the end products are $FeCl_2$ and CuCl. CuCl is insoluble in water, whereas $FeCl_2$ is soluble. If necessary, the mixture of these two components can be separated by this means, and each can be recycled to its use point.

Although the CuCl reaction scheme does provide essentially complete conversion of $FeCl_3$ to $FeCl_2$, the replacement of one reaction by these two staged reactions is not desirable because it involves additional energy consumption.

7) $$FeCl_2 + H_2 \rightarrow Fe + 2HCl$$

Figure 3 shows that the free-energy change for Reaction 7 decreases with increasing temperature, but is still slightly positive even at 925°C. The reaction does proceed, however, at 800° to 925°C with excess hydrogen flow. We find 90% conversion in 2 hours at 800°C; the other 10% of the $FeCl_2$ does not react only because it sublimes from the reaction zone to a colder section of the reactor.

HALOGEN RECYCLE

Reactions 8 and 9 are the reduction of halogen or the oxidation of halogen acid. The reverse-Deacon and Deacon reactions are the method for recycling halogen or halogen acid and thereby closing each cycle. The reverse-Deacon (Reaction 8) is particularly important in thermochemical hydrogen production cycles; it is the oxygen-liberating step in 17 of the cycles we have examined experimentally. As Figure 4 illustrates, the reverse-Deacon reaction is favored above 590°C, and the Deacon reaction is favored below this temperature.

8) $$Cl_2 + H_2O \rightarrow 2HCl + 1/2O_2$$

Because the reverse-Deacon reaction is completely homogeneous, a simple, heated ceramic tube with cooled exit line was utilized as the reactor. For a mixture of chlorine with excess steam, conversion, based on chlorine, varied from 92% to 98% for the temperature range 700° to 900°C. Apparently the reaction attains near-equilibrium conversions at these temperatures, even without a catalyst. As illustrated by the reaction free-energy changes (Figure 4), the equilibria are quite favorable. Thus, only a slight excess of steam is needed for complete conversion.

9) $$2HCl + 1/2O_2 \rightarrow Cl_2 + H_2O$$

The Deacon reaction is a well-known industrial process(18) and its equilibrium and reaction-rate data are well documented. We verified operation at a temperature of 200°C without a catalyst, which parallels the operating conditions of the industrial processes with catalysts. A stoichiometric mixture of HCl and oxygen, passed through a reaction tube identical to that described above, was completely converted in 1 minute of residence time.

EFFICIENCY OF THE IRON-CHLORINE-HYDROGEN-OXYGEN GROUP OF CYCLES

From the nine reactions discussed above, we can construct five cycles that typify the iron-chlorine-hydrogen-oxygen group. In the IGT nomenclature system, these five cycles are denoted as A-1, A-2, B-1, B-2, and I-6. Table 4 lists the reaction steps (of Table 3) that constitute each cycle and the calculated "maximum attainable" efficiencies, assuming the reaction temperatures of Table 3.

Table 4. TYPICAL SET OF THE IRON-CHLORINE-HYDROGEN-OXYGEN GROUP OF CYCLES

IGT Cycle	Reaction Steps	"Maximum Attainable" Efficiency, %
A-1	1, 3, 6, 7, 8	40
A-2	1, 4, 6 (X 1.5), 7, 9	30
B-1	2, 3, 6, 8	47
B-2	2, 4, 6 (X 1.5), 9	35
I-6	3, 5, 6 (X 1.5)	47

Cycle B-1 has been independently derived by Abraham and Shreiner of Argonne National Laboratory (10), although they apparently have done no experimental work with it. Cycle I-6 is our designation for EURATOM's Mark-9 cycle (14), derived by Hardy of the EURATOM laboratory in Ispra, Italy; it is currently

the subject of continued work by that laboratory. Cycles B-1 and I-6 also have the highest "maximum attainable" efficiency of this group at 47%.

Using the experimentally determined conditions of operability for individual reactions, we can calculate a more realistic value of "maximum attainable" efficiency for these cycles. Because the intention of the experiments reported here is simply to determine reaction feasibility to differentiate workable from nonworkable cycles, mass-transfer and reaction rates have temporarily been given only secondary importance. Our reactor design, mass-transfer rate, and reactant surface area could be much improved for any specific reaction, and this would greatly enhance the observed kinetics and yields.

We have recalculated the "maximum attainable" efficiency for cycles B-1 and I-6 with reaction temperatures at known experimental operating conditions. This efficiency drops to about 43% for both cycles, versus the 47% calculated by assuming the thermodynamic optimum temperature conditions listed in Table 3.

CONCLUSIONS

Almost all known pure thermochemical hydrogen production cycles can be grouped into five generic classes, each involving either a metal oxide or a metal halide as an intermediate.

In general, those cycles with the highest-temperature endothermic reactions and the least number of reactions are the most efficient. This is expected because thermochemical cycles are special types of heat engines. The "maximum attainable" efficiency of known published cycles is about 65% with 1225°C input heat and assuming present technology for conversion of heat to work.

The most difficult step in any thermochemical cycle is usually the one involving a change in metal oxidation state, usually the reduction. It is often necessary to operate such a step with some work input, such as electrolysis. Because of this, few of the truly efficient and workable hydrogen production cycles are purely thermochemical.

Of those thermochemical hydrogen production cycles that are known to be workable with reagent-grade materials, more than two-thirds are of the group constructed from compounds of iron, chlorine, hydrogen, and oxygen. The "maximum attainable" efficiency for cycles of this group is about 47% with 925°C input heat and present technology for conversion of heat to work. This efficiency drops to about 43% if the reaction steps are assumed to operate at temperatures of proven workability rather than at theoretically optimum temperatures based on thermodynamics.

ACKNOWLEDGMENT

The author is indebted to John Sharer for his many technical contributions to this research program.

This research is part of Project IU-4-14,"Thermochemical Hydrogen Production," sponsored by the American Gas Association; Dr. A. Flowers of A. G. A. is the program manager. We gratefully acknowledge the continued support of the A. G. A. for development of this technology.

REFERENCES

1. Sharer, J. and Pangborn, J., "Survey of Programs on Thermochemical Hydrogen Production," Chapter 6 in Gillis, J. et al., Survey of Hydrogen Production and Utilization Methods, Vol. II of Institute of Gas Technology Report to NASA Marshall Space Flight Center, Huntsville, Ala., Contract No. NAS 8-30757, August 1975.

2. Bowman, M. G. et al., "Hydrogen Production by Low Voltage Electrolysis in Combined Thermochemical and Electrochemical Cycles." Paper presented at the 146th Meeting of the Electrochemical Society, New York, October 1974.

3. Brecher, L. E. et al., "Studies of the Use of Heat From High Temperature Nuclear Sources for Hydrogen Production Processes," NASA Lewis Research Center Report CR-134918, Tasks 1 and 2.

4. Pangborn, J. and Sharer, J., "Analysis of Thermochemical Water-Splitting Cycles,"in Veziroglu, T. N. Ed., Hydrogen Energy, 499-515. New York: Plenum Press, 1975.

5. Stull, D. R. and Prophet, H., JANEF Thermochemical Tables, 2nd Ed., NBS Publication No. NSRDS-NBS 37. U. S. Department of Commerce, June 1971.

6. Rossini, F. D. et al., Selected Values of Chemical Thermodynamic Properties, NBS Circular 500. U.S. Department of Commerce, February 1952.

7. Coughlin, J. P., Heats and Free Energies of Formation of Inorganic Oxides, Bureau of Mines Bulletin 542. Washington, D. C.: U. S. Department of Interior 1954 .

8. Wicks, C. E. and Block, F. E., Thermodynamic Properties of 65 Elements – Their Oxides, Halides, Carbides, and Nitrides, U. S. Bureau of Mines Bulletin 605. Washington, D. C.: U. S. Department of Interior 1963 .

9. Funk, J., "Thermodynamics of Multi-Step Water Decomposition Processes," Am. Chem. Soc. Div. Fuel Chem. 16, No. 4, 49-87 (1972).

10. Abraham, B. and Schreiner, F., "General Principles Underlying Chemical Cycles Which Thermally Decompose Water into the Elements," Ind. Eng. Chem. Fundam. 13, No. 4, 305-310 (1974).

11. Funk, J., Conger, W. and Carty, R., "Evaluation of Multi-Step Thermochemical Processes for the Production of Hydrogen From Water," in Veziroglu, T. N., Ed., Hydrogen Energy, 457-470. New York: Plenum Press, 1975.

12. Chao, R., "Thermochemical Water Decomposition Processes," Ind. Eng. Chem. 13, 94-101 (1974).

13. Fueki, K., "Application of Free Energy Diagrams to Thermochemical Processes," University of Tokyo, Japan, 1975.

14. DeBeni, G. et al., "Thermochemical Water-Splitting as a Method for Hydrogen Production." Paper III-17 of British Nuclear Engineering Society Meeting, London, November 1974.

15. Tarman, P. B., "Status of the Steam-Iron Program." Paper presented at 7th Synthetic Pipeline Gas Symposium, Institute of Gas Technology, Chicago, October 1975.

16. Institute of Gas Technology, Process Research Division, "HYGAS – 1972 to 1974," IGT Report 110, ERDA Report FE-1221-1. Washington, D. C.: U.S. Energy Research and Development Administration, July 1975.

17. Institute of Gas Technology, "Development of the Steam-Iron System for Production of Hydrogen for the HYGAS Process," Interim Report 1, OCR Contract No. 14-32-0001-1518, Chicago, August 1974.

18. Furusaki, S., "Catalytic Oxidation of Hydrogen Chloride in a Fluid Bed Reactor," AIChE J. 19, 1009-1016 (1973) September.

19. Bowman, M. G., "Thermochemical Production of Hydrogen From Water," Quarterly Report LA-5731-PR. Los Alamos, N. M., Los Alamos Scientific Laboratories, June 1974.

20. Pangborn, J. B., "Laboratory Investigations on Thermochemical Hydrogen Production." Paper presented at The First World Hydrogen Energy Conference, Miami Beach, March 1976.

Appendix. ANALYSIS OF Fe_2O_3/Fe_3O_4 MIXTURES

Because Fe_3O_4 contains 1 mole of Fe^{+2} per mole of oxide, the concentration of this oxide can be determined by measuring the concentration of Fe^{+2}. To dissolve a mixture of the oxides Fe_2O_3 and Fe_3O_4, a strong acid is required; unfortunately, Fe^{+2} is readily oxidized in a strongly acid solution. This problem can be circumvented by placing a known amount of a standard oxidizing agent, $K_2Cr_2O_7$, in the acidic solvent. As the oxides dissolve, the Fe^{+2} is quantitatively oxidized in situ. Thus, the concentration of Fe^{+2} can be determined indirectly by a back titration with a standard Fe^{+2} solution to measure the unreacted portion of the standard oxidizing agent.

The concentration of Fe_2O_3 in the sample is determined indirectly by measuring the total iron concentration via a potassium dichromate titration. After the quantity of iron present as Fe_3O_4 has been subtracted (this would be 3 times the Fe^{+2} concentration), the concentration of Fe_2O_3 can be calculated.

The above procedure can also be applied with slight modification to Cu_2O/CuO mixtures. The determination of Cu^{+} is identical to the procedure for Fe^{+2}. The total copper concentration, however, is determined by an EDTA titration.

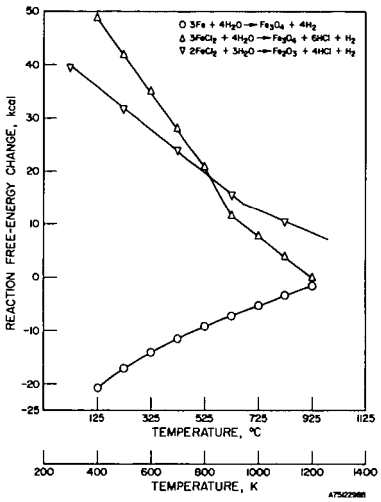

Figure 1. FREE-ENERGY CHANGE FOR THE METAL OXIDATION REACTIONS

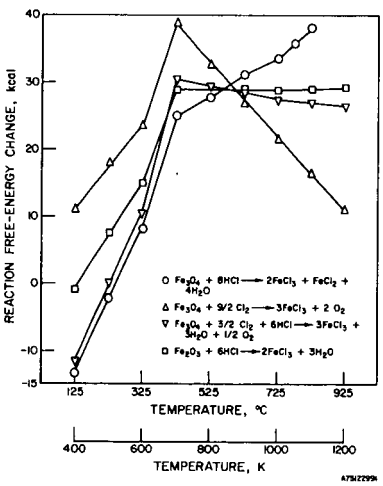

Figure 2. FREE-ENERGY CHANGE FOR THE METAL HALOGENATION REACTIONS

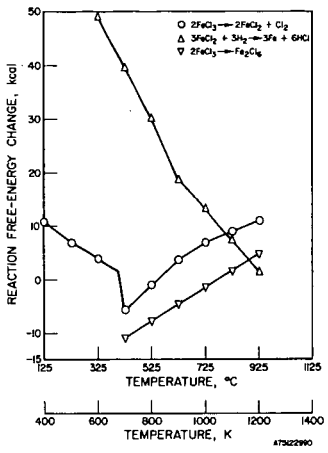

Figure 3. FREE-ENERGY CHANGE FOR THE METAL REDUCTION REACTIONS

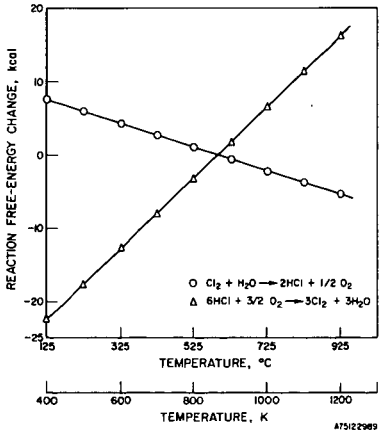

Figure 4. FREE-ENERGY CHANGE FOR THE HALOGEN RECYCLE REACTIONS